Development, Modeling and Control of a Novel Design of Two-Wheeled Machines

K M Goher [1] and M O Tokhi [2]
[1]Department of Mechanical and Industrial Engineering
College of Engineering, Sultan Qaboos University, Oman, e-mail: kgoher@squ.edu.om
[2]Department of Automatic Control and Systems Engineering,
The University of Sheffield, United Kingdom

***Abstract*- As far as the system of two-wheeled machine is concerned, incorporating a linear actuator to the intermediate body (IB) of two - wheeled vehicles has not presented in literature before. This paper investigates development, modeling and control of a novel design of a two wheeled vehicle with additional mobility features allowing an attached payload to move vertically while maintaining the entire system balance condition. This work aims to develop and build a well designed two-wheeled vehicle with specific features. Certain mechanical issues are discussed in order to build a well designed mechanical prototype. The prototype is designed so as to be able to carry and move a payload in a vertical direction while maintaining a balance condition of the vehicle on two wheels. An approach for modeling the system to characterize its dynamic behavior is also presented. A control strategy is developed and implemented on the system in order to steer the vehicle to perform a certain wheels trajectory. Different wheel trajectory profiles are used to check the capability of the developed control scheme to tackle the control problem while maintaining the balance condition of the entire mechanism.**

Keywords:* *Inverted pendulum, Two wheeled vehicle, Lagrangian dynamic formulation, PID control

I. INTRODUCTION

The research on balancing two-wheeled robots has gained momentum over the last decade in a number of robotics laboratories around the world. This is due to the inherent unstable dynamics of such systems. The control quality of such robots is characterized by the ability to balance on its two wheels and provide spin on the spot. This additional maneuverability allows easy navigation on various terrains, turn at sharp corners and traverse small steps or curbs. These capabilities have the potential to solve a number of challenges in industry and society. For example, a motorized wheelchair utilizing this technology would give the operator greater maneuverability and thus access to places most able-bodied people take for granted. Small carts built utilizing this technology allow humans to travel short distances in a small area or factories as opposed to using cars or buggies which are more polluting. The rapid increase of the aged population in countries like Japan has prompted researchers to develop robotic wheelchairs to assist an elderly to move around, (Takahashi et al. 2000). Two-wheeled machines have different applications due to their advantages which arise from their special design. For example, a two wheeled vehicle may be safer for the occupants while simultaneously being more agile to navigate narrow city streets. Furthermore, the reduced volume and lower mass of this configuration would increase fuel efficiency and overall functionality.

Choi *et al*. developed a wheeled inverted pendulum and investigated the interaction between human and the robot through applying a pulling or pushing force. They developed a control algorithm able to move and stabilize the robot in coordination with the external force of a human. Imamura *et al*. discussed the configuration of a baggage transportation system by an inverted pendulum robot and realized a navigation system. Jeong and Takahashi discussed the mobile control and the standing and sitting motions of an inverted pendulum type assistant robot aiming at the coexistence of safety and work capability. Jingtao *et al* discussed the mechanical design and dynamic modeling of a differential drive two-wheeled inverted pendulum mobile robot, which has the advantage of high maneuverability on slopes and narrow spaces and is able to carry human beings as well as other goods. Nawawi *et al*. designed and developed a two wheeled inverted mobile robot for use as flexible platform, comprising an embedded unstable linear plant intended for research and teaching purposes. Through this work, issues such as selection of actuators and sensors, signal processing units, modeling and control scheme have been addressed and discussed. Zheng *et al* discussed the mechanical design and control system of a miniature autonomous surveillance robot ("BMS-1") for indoor reconnaissance tasks.

Most of the work found in the area concentrated on developing the control algorithms required to keep the two-wheeled inverted pendulum robot in a balancing state. Other works discussed the dynamics of the system. The paper presents a two wheeled robot with an additional degree of freedom along its intermediate body to provide a payload with the ability to reach different heights. Furthermore, mathematical modeling of the dynamic behavior of the robot is also presented.

The aim of this work is to develop a new design of two-wheeled machines able to carry a payload while maintaining the balance condition in the upright position. The payload motion is incorporated by considering adding a linear actuator in order to activate the payload to move along the intermediate body with appropriate speeds. The intermediate body of the vehicle is considered to be a combination of two co-axial parts connected by the linear actuator. Adding a new actuator to the system adds additional degree of freedom along the intermediate body.

The paper is organized as follows: Sections II and III describe the system design procedures used and an investigation on different aspects of the vehicle design process where a detailed description of the test rig mechanical and electronic parts is introduced. Section IV carries out a mathematical description of the new

developed vehicle utilizing Lagrangian-based approach to derive the system equation of motion. Section V introduces the developed control approach to achieve a balance condition of the vehicle in the upright position. A numerical simulation analysis is carried out in section V by implementing the developed control strategy into the mathematical model of the vehicle.

II. DEVELOPMENT OF THE REAL PROTOTYPE

Rather than dealing with virtual motion of a payload attached to the intermediate body of the vehicle as presented by Goher and Tokhi, a real payload motion is considered in this work. The intermediate body is considered to consist of two coaxial parts connected by a mechanical linear actuator as shown in Figure 1. The actuator is considered to activate the payload in order to move along the intermediate body with prescribed motion characteristics.

The design objective is to build a novel robotic two wheeled platform capable of performing in narrow spaces and on slopes while carrying a payload at different positions and with the attitude of moving vertically. The main target of the design includes achieving a compact, high load capacity and light weight without scarifying the entire robot stiffness.

The mechanical design targets the following main features:

- A symmetrical mass distribution for the entire robot parts and components.
- Light weight without affecting the robot stiffness.
- Compactness with offering proper rooms for system electronics and accessories.
- Two auxiliary wheels-supports for safety operation and emergency fall over.

A. Vehicle main parts

The vehicle with an extended rod is considered to constitute the following parts:

- Two wheels for driving and manoeuvering connected by axle of length H ,
- Two DC motors driving the wheels located at the connection between the wheels and the connecting axle.
- The two motors are considered to act independent of one another; produce different torques in case of manoeuvering the vehicle which results in rotating the wheels by different velocities. However, they produce the same torque if a forward/backward linear motion is assigned to the vehicle.
- If the two control signals are the same in magnitude and direction the wheels will rotate in the same direction with the same speed which results in a forward/backward linear motion.
- If the two control signals are the same in magnitude but in opposite directions the wheels will rotate with the same speed but in different directions which in turn cause the vehicle to rotate according to speeds of the wheels.
- The intermediate body consists of two coaxial parts connected by a linear actuator.
- The lower part of mass M_l is connected at its lower end to the wheels axle with a rigid joint and to the linear actuator at the upper end.
- The upper part of the intermediate body is of mass M_u and is connected to a payload of mass M at the upper end.

The work introduces a two wheeled vehicle with an additional feature and a linear translational degree of freedom. The proposed prototype sketched using the (*Pro Engineer wildfire 4.0*) is shown in Fig. 1. The design has two main wheels driving the vehicle which allow it to manoeuvre around. Other two auxiliary wheels are attached to the front and rear of the robot the robot safety to prevent it from falling off. The other main part of the vehicle is the intermediate body (IB) of the vehicle which is composed of two co-axial parts connected by a linear actuator with a payload attached to the end of the upper part. The linear actuator allows the payload to move up and down along the vehicle intermediate body (IB), and this adds an additional translational degree of freedom. The robot thus is a four-degree-of-freedom system. With such design, the system is still under actuated as the number of actuated axes is less than the resulting independent motion achieved.

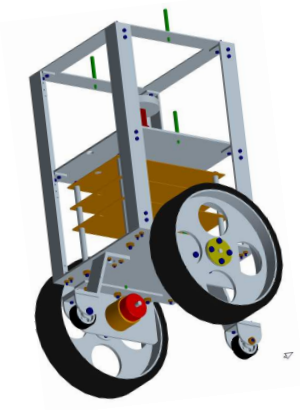

Fig. 1 Pro Engineer design of the prototype

A real test rig, shown in Figure 2 and 3, has been designed and developed in the Automatic Control and Systems Engineering department, University of Sheffield, based on the developed design. The test rig is currently in the testing stage and verification of the mathematical model with the experimental setup will appear in future work.

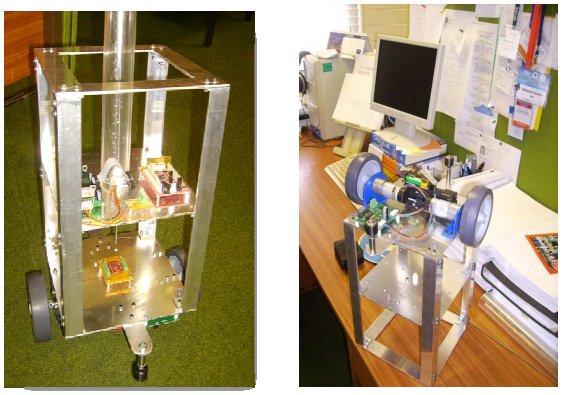

Fig. 2 Real test rig, ACSE department, University of Sheffield

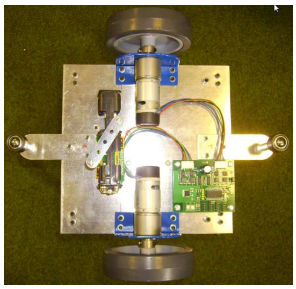

Fig. 3 Bottom view of the test rig base

B. Mechanical components and parts

This comprises an Aluminum structure with four right-handed angles in each side. Those four angles are used to support the base plate attached to the two main deriving motors, the intermediate plate carrying the linear actuator and the upper plate. The base plate of the test rig is supported by means of two auxiliary rollers attached at both sides of the base plates. The auxiliary rollers are used to provide a support for the vehicle and additional safety precautions in case of control scheme failure or inappropriate work which may cause the whole system to collapse. In the real development of the test rig, the rollers are used to the replace the two auxiliary wheels shown in Figure 1; depending on wheels will add constraints to the entire system in maneuvering and rotating specifically in rough terrains. Two main 100 mm diameter 5 mm hub wheels, shown in Figure 4, are used to provide the vehicle with motion.

Fig. 4 100 mm diameter wheel with 5 mm hub

C. Electronic components and accessories

Two DC permanent magnet motors, shown in Figure 5, are used drive the vehicle with their technical specifications available in Table 1. Each motor is provided with a built-in shaft encoder with 360 counts/shaft revolution.

Fig. 5 EMG30 and Mounting Bracket

A 12v 2.8A Dual H-Bridge motor controller, shown in Figure 6, is utilized. This motor driver is designed to work with the EMG30 gear motors; the MD25 will drive two motors. It can be controlled by serial or the I2C Interface. There are two modes of operation; direct individual control of the motors or the ability to send a speed and a turn commands.

TABLE 1: Motor technical specifications

Specification	**Parameter**	**Units**
Voltage	12	*Vdc*
Torque	1.5	*Kg.cm*
Max. speed	170	*rpm*
Max. current	530	*mA*
No load speed	216	*rpm*
No load current	150	*mA*
Stall current	2.5	*A*
Rated power	4.22	*W*
Encoder counts/rev	360	*counts*

Fig. 6 Motor driver, 12v 2.8A Dual H-Bridge

In order to provide the attached payload with the required sliding motion, a screw thread driver, shown in Figure 7, is used. The linear actuator is able to hold a weight of more than 1.3 kg while travelling through a maximum stroke of 48mm. The full technical specifications of the screw driver are shown in Table 2.

Fig. 7 Screw thread driver

TABLE 2: Screw thread driver technical specifications

Specification	**Parameter**	**Units**
Voltage	12	*Vdc*
Torque	1.5	*Kg.cm*
Holding force	13.3	*N*
Max. travel	48	*mm*
Step angle	7.5	deg*ree*
Step/rev	48	*mm*
Diameter – body	26.16	*mm*
Diameter – shaft	3.43	*mm*
Lead length	304.8	*mm*
Mounting hall spacing	34.9	*mm*
Max. current	530	*mA*
No load speed	216	*rpm*
No load current	150	*mA*
Stall current	2.5	*A*
Rated power	4.22	*W*
Encoder counts/rev	360	*counts*

As can be noticed from Table 2, the shaft diameter of the screw thread will not be able to support the continuous motion of the attached payload. A

transparent tube of 40 mm outside diameter is attached vertically to the intermediate Aluminum board. The tube provides the payload, attached to the screw thread, with the necessary support and guidance while moving up/down due to the actuation provided by the linear actuator.

An Atmel microcontroller ATmega32, 32-Kb self-programming flash program memory, 2-Kb SRAM, 1-K EEPROM, 8 channel 10-bit A/D-converter. JTAG interface for on-chip-debug. Up to 16 MIPS throughput at 16 Mhz, shown in Figure 8, is used.

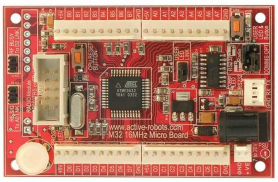

Fig. 8 Atmel microprocessor

The M32 board is Radio Ready and can be easily upgraded with an easy radio transceiver module. Using the radio link, the M32 board can communicate with a PC or any computer with a serial link and be controlled without wires making it ideal for remote control and data logging applications.

A compact SCA3000 triple axis accelerometer, shown in Figure 13, is used.

This accelerometer is highly precise and temperature compensated which is an efficient option specifically for IMU and dead-reckoning applications. The low noise and temperature compensation significantly reduces drift over time. SCA3000-D01 has an easy to use SPI interface. This breakout board includes a low noise, low drop out, 3.3V regulator that accepts voltages from 3.35V to 10V.

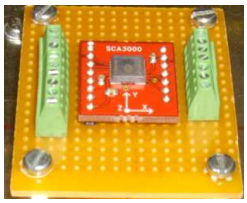

Fig. 9 Accelerometer, SCA 3000

III. DESIGN TECHNICAL CONSIDERATIONS

Certain design aspects are considered in the design process of the prototype, this section is discuss that in detail:

A. Design of the inclination angle

As the vehicle starts working from rest, the vehicle leans to the floor on three wheels as shown in Fig. 10; two main wheels and one of the auxiliary wheels. As the auxiliary wheel touches the floor, its centre rotates from position O_a to position O'_a which in turn causes the entire vehicle to shift with an angular position θ_o from the upright vertical position.

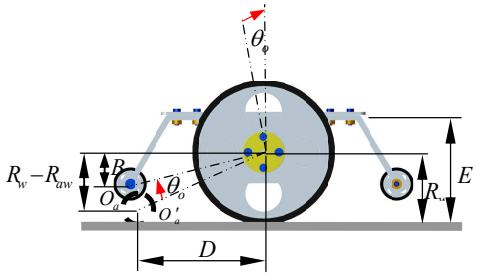

Fig. 10 Vehicle angle of inclination (stand up angle)

The angle of inclination θ_o can be derived based on the geometry of the developed vehicle design as:

$$\theta_o = \tan^{-1}\left(\frac{R_w - R_{aw}}{D}\right) - \tan^{-1}\left(\frac{B}{D}\right) \quad (1)$$

where R_w is the main wheel radius, R_{aw} is the auxiliary wheel radius, D and B are the horizontal and vertical distances of the centre of the auxiliary wheel from the centre of the main wheel respectively. For such design, θ_o will constitute a design specification for the vehicle to stand up. Such angle should be considered when designing driving motors of the wheels as the driving torque necessary for lifting the vehicle to the upright position will depend on the value of this angle.

B. Vehicle static balancing

For the vehicle in a steady situation, the following conditions are applied:

- No control strategy works and hence no force or moment applies except that resulting from the vehicle gravitational force; $M_{eq}g$.
- Both the main wheels and one of the auxiliary wheels are resting on the floor.
- No linear acceleration for the vehicle; $\ddot{X} = \ddot{Y} = 0$.

With the vehicle standing on three wheels, as shown in Figures 11 and 12, the summation of the reaction forces, in a vertical direction, at those wheels constitute the only force acting in that position, which is equal to the vehicle gravitational force;

$$\sum Forces_Z = M_v g$$
$$F_1 + F_2 + F_3 = M_v g$$
$$2F + F_3 = M_v g \quad \text{and} \quad (F_1 = F_2 = F) \quad (2)$$

Where

$$M_v = M_c + (M_l + M_a + M_u + M) \quad (3)$$

For a static scenario of the vehicle on three wheels, there is no translational or rotational motion;

$$\sum F_Z = 0 \qquad (\ddot{Y} = \ddot{Z} = 0)$$
$$\sum M_{C1} = \sum M_{C2} = 0 \qquad (\omega_x = 0)$$

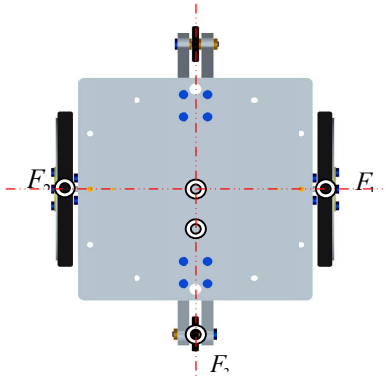

Fig. 11 Plan of the vehicle with wheels reaction forces

Applying the previous conditions, one can obtain the following expressions:

$$\sum M_{C1} = 0$$

$$F_3 = \frac{L_g \sin\theta_o \cdot M_v g}{D} \quad (4)$$

From equation (1),

$$F = \frac{1}{2} M_v g \left(1 - \frac{L_g \sin\theta_o}{D}\right) \quad (5)$$

C. Vehicle fall over calculations

For safety considerations of the vehicle, much interest is carried out on the conditions which may lead to the vehicle falling down from its standing position on three wheels. The importance of such study is to help in designing the angle θ_o and suitable geometry of the related dimensions such as R_w , R_{aw} , D , and B .

For the wheel to be reliable to falling over, the following conditions apply:

- There is no reaction force at the main wheels and floor interaction as they are not touching it all;
- $F_1 = F_2 = F = 0$

Position of the auxiliary wheel C_3 represents a point of the vehicle falling over and hence the moment if applied will lead to such situation.

$$\sum M_{C3} = M_v g\left(D - L_g \sin\theta_o\right) \quad (6)$$

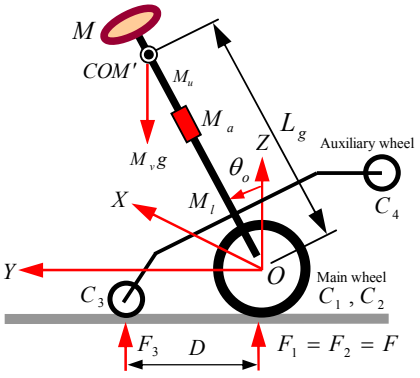

Fig. 12 Stand condition of the vehicle on three wheels

D. Starting moving from standing calculations

Carrying out force calculations due to the gravitational force of the vehicle in two directions; perpendicular and parallel to the direction of the vehicle intermediate body (IB) yields:

$$\sum F_{\perp} = M_v g \sin\theta_o$$

$$\sum F_{//} = M_v g \cos\theta_o$$

where $\sum F_{\perp}$ and $\sum F_{//}$ are the forces acting on the vehicle due to its own weight perpendicular and parallel to the direction of the IB.

If an external force F_{ex} is applied to the vehicle it might cause it to move forward or backward according to the following conditions:

- The vehicle starts to move forward the auxiliary wheel at position C_3 if
  $F_{ex} < F_{\perp}$ (7)
- The vehicle starts to move backward towards the main wheels at position C_1 and C_2 if
  $F_{ex} < F_{//}$ (8)
- The vehicle remains stationary at its position if
  $F_{ex} \geq F_{//}$
  $\geq F_{\perp}$ (9)

IV. SYSTEM MODELING

The two-wheeled robotic vehicle considered in this work comprises a rod on an axle incorporating two wheels as described in Figures 5 and 6. The robot is powered by two DC motors driving the vehicle wheels and a linear actuator connecting the two parts of the IB which allows the attached payload to move up and down according to a pre described motion scenario. A reference Cartesian coordinate frame designated as $OXYZ$ attached to the axle connecting the wheels with its origin located at the vehicle centre point O as shown in Figures 1 and 2 is used for the angular and translational motion of the vehicle. The $Z-$ axis points vertically upward, the Y axis is parallel and coincides with the wheels axle, and the axis is determined according to the right-hand rule in the rectangular coordinate system. The IB is considered balanced if it coincides with the positive $Z-$ axis. Partial angular deviation from the Z axis causes an imbalance in the vehicle with a tilt angle θ_p around the X axis.

A. Effect of adding a linear actuator

A linear actuator of mass M_a is used to activate the upper part of the intermediate body and the attached payload. As a result of the actuation, the upper part of the IB and the attached payload with experience a linear motion, along the intermediate body, with a displacement Q as shown in Figure 5.2. Due to such motion, the positions of the centres of mass L_u and L_M will depend on the variable Q and in turn the position of the entire COM of the intermediate body L_g .

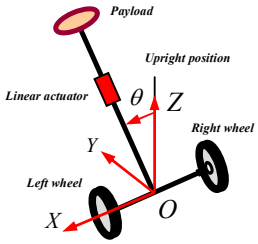

Fig. 13 Two-wheeled vehicle with an extended rod

B. Corriolis effect due to the linear actuator

Due to the simultaneous translational motion exerted by the linear actuator along the intermediate body and the partial rotational motion of the intermediate body, both the upper part of the rod, represented by a mass M_u, and the attached payload M will have a Coriolis component of acceleration which can be represented respectively by the following expressions:

$$a_{uc} = 2\dot{\theta}\frac{d}{dt}\left(2L_l + L_u + Q\right) \tag{10}$$

And

$$a_{uc} = 2\dot{\theta}\frac{d}{dt}\left(2L_l + 2L_u + Q\right) \tag{11}$$

The Coriolis force due to those accelerations can be expressed as the following:

$$F_{cor} = 2\dot{\theta}\left(M_u\frac{d}{dt}\left(2L_l + L_u + Q\right) + M\frac{d}{dt}\left(2L_l + 2L_u + Q\right)\right) \tag{12}$$

Due to the effect of this force, both the attached payload and upper part of the rod appear to deflect from the path of motion.

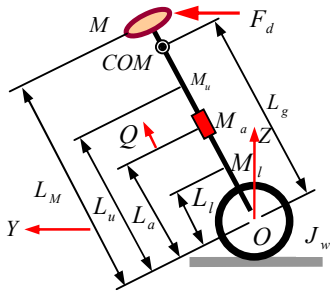

Fig. 14 Positions of vehicle main parts and *Com*

B. Steering kinematics

The equations describing the differential driving system can be used to predict how a robot equipped with such a system will respond to changes in its wheel speed and what path it will follow under various conditions. The equations can also be used to calculate a robot's position in dead-reckoning or localization by odometry applications; techniques that estimate a robot's position based on distances measured with odometer devices mounted on each wheel.

In any kinematics description approach, the causes of motion are ignored and the core of the investigation is the resulting motion itself. The equations derived in this section describe the robot's position and orientation as a function of the movement of its wheels, but ignore the underlying physics resulting in the corresponding motion. Issues such as torques and forces, friction, energy and inertia will be left for the dynamics of the vehicle steering.

The mathematical model of the vehicle is developed based on the kinematic and dynamic relations of the system. Control algorithms are designed and implemented to control the vehicle while steering. Maintaining the vehicle balanced during steering is a crucial mission of the control technique.

The derivation of the robot trajectory is based on the following assumptions:

- The vehicle is considered as a rigid body and hence all the vehicle points undergo the same change of orientation.
- The wheels are travelling at different speeds; otherwise their trajectory equations are trivial.
- A frame of reference $OXYZ$ is considered to be attached to the centre of the vehicle.

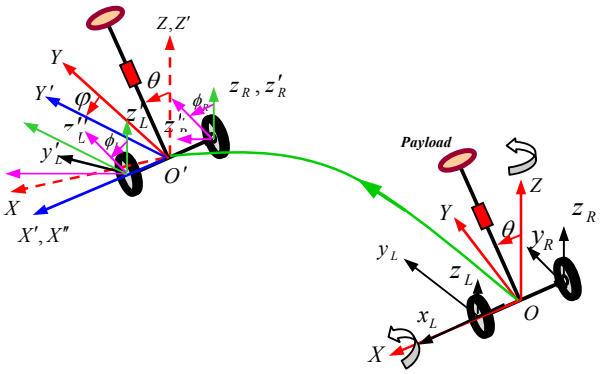

Fig. 15 Vehicle steering and path tracking diagram

Steering of the vehicle is carried out by a couple of rotations, described in Figures 15 and 16, of the system wheels as follows:

- Rotation about the X axis for the left and right wheels with δ_L and δ_R respectively.
- Rotation about the Z axis with an angle ϕ.

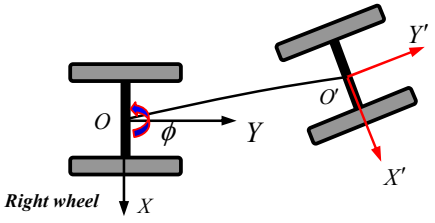

Fig. 16 Schematic diagram of the vehicle wheels

Hence, the angular velocities of the left and right wheel will be a vector summation of the two previously mentioned rotations as follows:

$$\underline{\omega}_L = \underline{\dot{\phi}} + \underline{\dot{\delta}}_L \tag{13}$$

$$\underline{\omega}_R = \underline{\dot{\phi}} + \underline{\dot{\delta}}_R \tag{14}$$

The angular velocity of the entire vehicle around the Z axis, due to the resulting yaw angle ϕ, shown in Figure 4, can be expressed as

$$\dot{\phi} = \frac{R_w}{H}\left(\dot{\delta}_R - \dot{\delta}_L\right) \quad (15)$$

Integrating equation 3, considering $\phi(0) = \phi_o$ as initial orientation of the vehicle, leads to an equation describing the vehicle orientation in terms of the wheels' velocities and the vehicle geometry as:

$$\phi(t) = \frac{R_w}{H}\left(\delta_R - \delta_L\right) + \phi_o \quad (16)$$

The velocity relation for the vehicle centre point O can be expressed in terms of the angular positions of the left and right wheels and the wheel geometry as:

$$\dot{Y} = \frac{1}{2} R_w\left(\dot{\delta}_L + \dot{\delta}_R\right) \quad (17)$$

The instantaneous position of the vehicle, expressed in the $OXYZ$ frame of reference, relies mainly on the velocity of the vehicle centre of mass (*COM*), and can be expressed as:

$$\frac{dX}{dt} = \frac{1}{2} R_w\left(\dot{\delta}_L + \dot{\delta}_R\right)\cos\phi(t) \quad (18)$$

$$\frac{dY}{dt} = \frac{1}{2} R_w\left(\dot{\delta}_L + \dot{\delta}_R\right)\sin\phi(t) \quad (19)$$

Considering the initial position of the vehicle as $X(0) = X_o$ and $Y(0) = Y_o$ and integrating yield the vehicle position as a function of time;

$$X(t) = X_o + \frac{1}{2} H \frac{\left(\dot{\delta}_L + \dot{\delta}_R\right)}{\left(\dot{\delta}_R - \dot{\delta}_L\right)}\left(\sin\left(\frac{1}{2} R_w\left(\dot{\delta}_R - \dot{\delta}_L\right)t/H + \phi_o\right) - \sin\phi_o\right) \quad (20)$$

$$Y(t) = Y_o + \frac{1}{2} H \frac{\left(\dot{\delta}_L + \dot{\delta}_R\right)}{\left(\dot{\delta}_R - \dot{\delta}_L\right)}\left(\cos\left(\frac{1}{2} R_w\left(\dot{\delta}_R - \dot{\delta}_L\right)t/H + \phi_o\right) - \cos\phi_o\right) \quad (21)$$

Vehicle Rotational position (Yaw Angle)

As a result of the partial rotation of the left and right wheels, the vehicle will start to spin about the vertical Z axis with degree of rotation called the yaw angle, ϕ. The difference between the torques of the wheels is the main source of the vehicle spinning. However, this rotational motion is resisted by the amount of frictional moment between the wheels and the ground. The angular acceleration of the entire vehicle due to a rotation about the Z axis can be obtained as

$$\ddot{\phi} = \frac{1}{J_{eqv}}\left(\frac{H}{2}\left(F_L - F_R\right) - M_{fg}\right) \quad (22)$$

The frictional moment M_{fg} represents the frictional resistance due to the interaction between the wheels and the ground and can be modelled according to Coulomb friction model as:

$$M_{fg} = c_v\dot{\phi} + c_c \sin\dot{\phi} \quad (23)$$

where F_d is the disturbance force, M_{fg} is the friction moment at the wheel ground interface, c_v and c_c are the viscous and Coulomb friction coefficients respectively and J_{eqv} is the equivalent moment of inertia of the entire vehicle about the Z axis.

B. Vehicle Lagrangian dynamics

Using Lagrange dynamic formulation for the system dynamics, the following dynamic equation can be expressed

$$\frac{dq}{dt}\left(\frac{\partial L}{\partial \dot{q}_i}\right) - \frac{\partial L}{\partial q_i} = Q_i \quad (24)$$

The generalized coordinates of the system are chosen as $q_i = [\delta_L \quad \delta_R \quad \theta \quad Q]^T$ and the generalized force is expressed as $Q_i = [F_L \quad F_R \quad F_d \quad F_a]^T$, where $L = T_v - V_v$, is the Lagrangian function, Q_i is a generalized force, and q_i generalized coordinate , δ_L and δ_R are the angular displacements of the left and right wheels around the X axis respectively, θ is the angular displacement of the IB, Q is the linear displacement of the payload along the IB, F_L and F_R are the driving forces of the left and right wheels respectively, F_d is an external disturbance force, and F_a is the linear actuator force.

System Energy Requirements

Estimation of the system energy requirements is of great importance in terms of the cost requirements, the design of the appropriate actuators and the development of suitable controllers.

The total energy, U of the vehicle can be described as the sum of the kinetic energy, T , and potential energy, V , of the system components; cart, lower and upper parts of IB, and the payload as:

$$U = T + V \quad (25)$$

$$T = T_c + T_l + T_a + T_u + T_M \quad (26)$$

$$V = V_l + V_a + V_u + V_M \quad (27)$$

$$T_c = \frac{1}{2} M_c \dot{Y}^2 \quad (28)$$

where

$$M_c = 2M_w + M_a + 2M_{motor} + 2M_{gearbox} \quad (29)$$

The pendulum kinetic energy can be expressed as the sum of its translational energy and rotational energy;

$$T_l = \frac{1}{2} M_l\left(\left(\dot{Y} + L_l\dot{\theta}\cos\theta\right)^2 + \left(L_l\dot{\theta}\sin\theta\right)^2\right) + \frac{1}{2} J_l\dot{\theta}^2 \quad (30)$$

$$T_l = \frac{1}{2} M_a\left(\left(\dot{Y} + L_a\dot{\theta}\cos\theta\right)^2 + \left(L_a\dot{\theta}\sin\theta\right)^2\right) + \frac{1}{2} J_a\dot{\theta}^2 \quad (31)$$

$$T_u = \frac{1}{2} M_u\left(\dot{Q}^2 + \left(\dot{Y} + L_u\dot{\theta}\cos\theta\right)^2 + \left(L_u\dot{\theta}\sin\theta\right)^2\right) + \frac{1}{2} J_u\dot{\theta}^2 \quad (32)$$

$$T_M = \frac{1}{2} M_M\left(\dot{Q}^2 + \left(\dot{Y} + L_M\dot{\theta}\cos\theta\right)^2 + \left(L_M\dot{\theta}\sin\theta\right)^2\right) + \frac{1}{2} J_M\dot{\theta}^2 \quad (33)$$

where J_l, J_a, J_u and J_M are the mass moments of inertia of the lower rod, linear actuator, upper rod and the payload respectively around the IB centre of mass.

The linear velocity of the vehicle centre point $\dot{Y}$ can be expressed as follows:

$$\dot{Y} = \frac{R_w}{2}\left(\dot{\delta}_L + \dot{\delta}_R\right) \tag{34}$$

Since there is no motion for the vehicle in the Z direction as the wheels remain in full contact with the ground; $\ddot{Z}_R = \ddot{Z}_L = \ddot{Z}_O = 0$, there is no potential energy for the cart in the Z direction. The potential energy of various components can be expressed as:

$$V_l = M_l g L_l \cos\theta \tag{35}$$

$$V_a = M_a g L_a \cos\theta \tag{36}$$

$$V_u = M_u g L_u \cos\theta \tag{37}$$

$$V_M = M g L_M \cos\theta \tag{38}$$

The potential energy of the vehicle can be obtained by summing equations (35), (36), (37) and (38) yielding:

$$V_{Vehicle} = M_{eq} L_g g \cos\theta \tag{39}$$

where L_g is the position of centre of mass (*COM*) of the IB, and it is time-dependent varying with the linear actuator displacement Q and can be calculated using;

$$L_g = \frac{1}{M_{eq}}\left[C + (M_u + M)Q\right] \tag{40}$$

where

$$M_{eq} = M_l + M_a + M_u + M \tag{41}$$

Manipulating the above equations yield the following two expressions for the total kinetic and total potential energies respectively of the system;

$$\begin{aligned} T_v = {} & \frac{1}{2}(2J_w + J_{IB})\dot{\phi}^2 + \frac{1}{2}C_9\dot{Q}^2 + \frac{1}{2}R_w\left[C + C_9 Q\right]\left(\dot{\delta}_L + \dot{\delta}_R\right)\dot{\theta}\cos\theta \\ & + \frac{1}{2}\left(C_{22} + C_{20}Q + C_{21}Q^2\right)\dot{\theta}^2 + \frac{1}{4}M_{eq}R_w^2\dot{\delta}_L\dot{\delta}_R \\ & + \left(\frac{1}{8}M_{eq}R_w^2 + M_w R_w^2 + J_w\right)\left(\dot{\delta}_L^2 + \dot{\delta}_R^2\right) \end{aligned} \tag{42}$$

$$V_v = \left[C + (M_u + M)Q\right] g \cos\theta \tag{43}$$

C. *Vehicle dynamic equations*

The lagrangian equations of motion of the vehicle can be represented as:

$$\frac{d}{dt}\left(\frac{\partial L}{\partial \dot{\delta}_L}\right) - \frac{\partial L}{\partial \delta_L} = F_L \tag{44}$$

$$\frac{d}{dt}\left(\frac{\partial L}{\partial \dot{\delta}_R}\right) - \frac{\partial L}{\partial \delta_R} = F_R \tag{45}$$

$$\frac{d}{dt}\left(\frac{\partial L}{\partial \dot{\theta}}\right) - \frac{\partial L}{\partial \theta} = F_d \tag{46}$$

$$\frac{d}{dt}\left(\frac{\partial L}{\partial \dot{Q}}\right) - \frac{\partial L}{\partial Q} = F_a \tag{47}$$

Manipulating the above expressions yields the following three non-linear differential equations describing the vehicle dynamics alongside the driving forces and the external applied force as:

$$\ddot{\delta}_L = \frac{1}{2C_{25}}\left(F_L - \frac{1}{2}R_w(C + C_9)\left(\ddot{\theta}\cos\theta - \dot{\theta}^2\sin\theta\right) - \frac{1}{2}C_9 R_w\left(\dot{Q}\dot{\theta} + Q\ddot{\theta} + \dot{Q}\cos\theta - Q\dot{\theta}\sin\theta\right) - C_{24}R_w^2\ddot{\delta}_R\right) \tag{48}$$

$$\ddot{\delta}_R = \frac{1}{2C_{25}}\left(F_R - \frac{1}{2}R_w(C + C_9)\left(\ddot{\theta}\cos\theta - \dot{\theta}^2\sin\theta\right) - \frac{1}{2}C_9 R_w\left(\dot{Q}\dot{\theta} + Q\ddot{\theta} + \dot{Q}\cos\theta - Q\dot{\theta}\sin\theta\right) - C_{24}R_w^2\ddot{\delta}_L\right) \tag{49}$$

$$\begin{aligned} \ddot{\theta} = {} & \frac{1}{\left(C_{22} + C_{20}Q + C_{21}Q^2\right)}\left(-\frac{1}{2}C_9 R_w\left(\dot{Q}\left(\dot{\delta}_L + \dot{\delta}_R\right) + Q\left(\ddot{\delta}_L + \ddot{\delta}_R\right) + \dot{Q}\cos\theta - Q\dot{\theta}\sin\theta\right) + F_d - \left(C_{20} + 2C_{21}Q\right)\dot{Q}\dot{\theta}\right. \\ & \left. + (C + C_9 Q)g\sin\theta - \frac{1}{2}R_w(C + C_9)\left(\ddot{\delta}_L + \ddot{\delta}_R\right)\cos\theta\right) \end{aligned} \tag{50}$$

$$\ddot{Q} = \frac{1}{C_9}\left(F_a + \frac{1}{2}\left(C_{20} + 2C_{21}Q\right)\dot{\theta}^2 + \frac{1}{2}C_9 R_w\dot{\theta}\left(\dot{\delta}_L + \dot{\delta}_R\right)\cos\theta - C_9 g\cos\theta\right) \tag{51}$$

V. CONTROL STRATEGY

The steering control strategy of the vehicle, shown in Figure 17, can be divided into two main sets of control loops; a set of three feedback controllers is responsible for stabilizing the vehicle in the upright position and a single control loop to control the attached payload position.

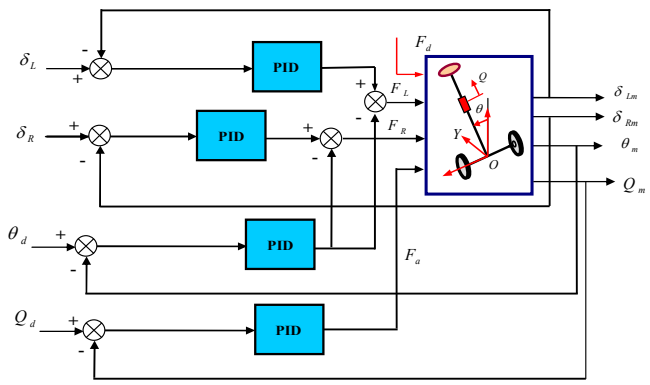

Fig. 17 Schematic description of the control strategy

Rather than depending on a single linear motion of the vehicle centre in one single direction, the steering of the vehicle, generally, relies on utilizing the rotation of both the left and right wheels to develop different control signals to activate the driving motors. Two separate feedback control loops are developed utilizing the partial angular position of each wheel and compared it to a desired angular motion trajectory of the corresponding wheel.

- Two controllers from the first set are used to control the amount of rotation of the left and right wheels. The error calculations for both control loops are based on the difference between the desired and actual measurements of both the wheels rotation.
- Investigation of the energy sufficient to steer the vehicle to the desired location is estimated for the entire course.

- The system outputs are the measurements of the angular position of the left and right wheels, the angular position (tilt angle) of the intermediate body and the displacement of the attached payload.
- The error and its time derivative for the yaw angle ϕ are the control inputs while the terminal voltage of the motor is the control effort required. Based on the measured instantaneous yaw angle of the vehicle, the orientations of both the left and right wheels are calculated.
- The third controller in this set is used to overcome the deviation in the intermediate body angular position around the target upright position.
- The error measurements resulting from the previous mentioned control loops are used as the inputs to the corresponding controller in order to create the appropriate control effort for the driving motors.
- The control signal resulting from the measurement of the intermediate body angular position is subtracted from both the control signals developed by the first two control loops.

VI. NUMERICAL ANALYSIS

As the vehicle is considered to be utilized for indoor and outdoor applications, it will be subjected or even forced to undergo various motion scenarios while performing a desired task or follow a specific trajectory. Three different trajectories are used to test the developed control techniques; partial finite angular movement of the wheels, two equal and opposite trajectories and a simple harmonic motion – like profile for each wheels.

A. Equal and opposite incremental angular position

As a simple test of the steering control strategy, the left and right wheels are considered to rotate in two opposite directions by 5 degrees (0.08721 radians). As a result, the vehicle will undergo a partial curvature motion with a curve length proportional to the amount of rotation of both wheels. Using a PD feedback control loop, the wheel's measured angular positions are fed back and compared to the desired angular position. The measured error is used to estimate the required control effort to drive each motor with the appropriate speed.

The control technique used was able to achieve the target orientation of the whole system within less than 10 seconds while achieving the system balance in the upright position as shown in Figures 18, 19, 20 and 21. The strategy showed the capability to control the system using feedback of both the angular orientations of the left and right wheels.

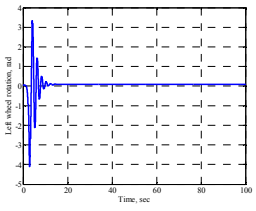

(a)

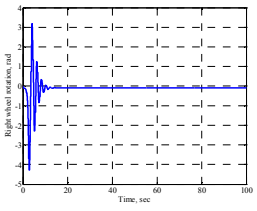

(b)

Fig. 18 Wheels angular motion

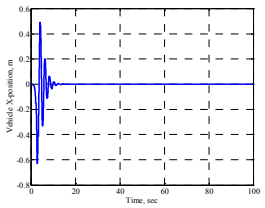

(a)

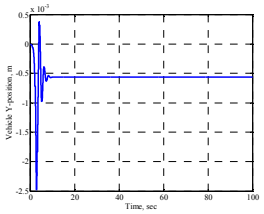

(b)

Fig. 19 Vehicle linear motion

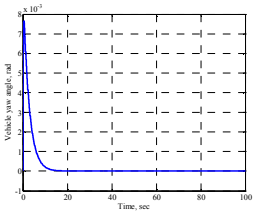

Fig. 20 Vehicle yaw angle

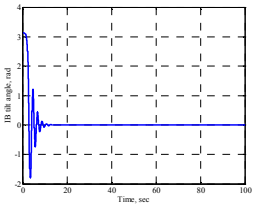

Fig. 21 IB tilt angle

B. Equal and opposite wheels trajectory

In this section, more complicated motion scenarios are assigned to the left and right wheels. Both wheels are expected to perform the following motion scenario:

- Starting rotation from rest, where the original position of the vehicle, with 1 degree, at a constant angular position of 0.1 rad/s until becoming stationary for 10 seconds.
- The wheels are accelerating again for a further 1 degree with the same speed until becoming stationary for the next 10 seconds.
- With a further rotation of 1 degree, the wheels are reaching the maximum allowable angular position where they are still stationary for 20 second before starting to rotate back to the original position.
- In order to return back to the original position, the wheels are allowed to be decelerated faster with a constant speed of 0.3 rad/s where they become stationary for the rest of the course.
- The above mentioned motion scenarios are conducted by both the left and right wheels in two opposite directions which allow the entire vehicle to undergo a planar motion in the X and Y directions and a rotational motion around the vertical Z axis.

Two PD control loops are developed to control the rotation of the left and right wheels where two control signals are required to activate the two driving motors activating the wheels. The control signal required mainly relies on the rate of rotation of each wheel.

The developed control strategy was able to track the desired reference signal, for both wheels, in around 10 seconds as shown in Figures 22(a) and 22(b). However, a big overshoot occurred in the transient period before settling down. The vehicle wheels, as mentioned in the motion scenario, are considered to encounter the same rate of rotation but in two opposite directions as noted in Figure 22 (c).

As the wheels rotated in the previous mentioned scenarios, the vehicle will undergo a planar motion. According to the kinematic equations 8 and 9 and due to the limited small rotation of the wheels, the linear motion of the vehicle is negligible in the X direction as shown in Figure 11. However, it is more noticeable in the Y direction; the vehicle is accelerated to move around the original position in the range of -0.6 – 0.5 meters where it is then decelerated in order to settle down within around 10 seconds.

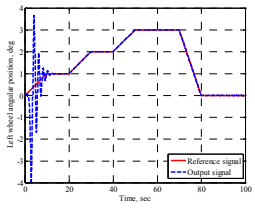

(a)

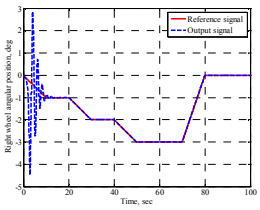

(b)

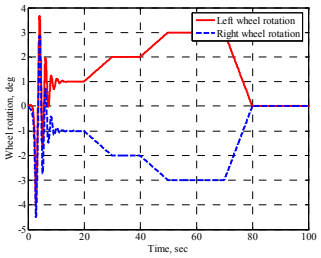

(c)

Fig. 22 Wheels angular motion, deg

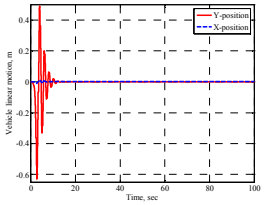

Fig. 23 Vehicle linear motion

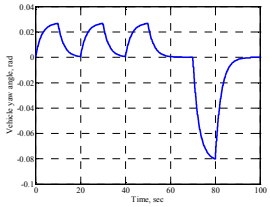

Fig. 24 Vehicle yaw angle

As a result of the successive periods of rotation of the two wheels, as mentioned above, the entire vehicle starts to rotate, as shown in Figure 24, about the vertical Z axis with a yaw angle ϕ proportional to the direction of rotation and the degree of rotation of both wheels.

The two wheels are accelerated to rotate in three consecutive periods; 0 - 10, 20 - 30 and 40 - 50 seconds, with the same constant speed of 0.1 rad/s in two opposite directions as shown in Figure 22 (a), (b) and (c). As a result, the vehicle undergoes the same yaw angle rotation. However, with a high speed of decelerating the wheels; 0.3 rad/s in the period between 70 and 80 seconds, the vehicle rotates in the opposite direction 4 times faster before readjusting itself to the original orientation in correspondence to the stationary wheels in the period from 80 -100 seconds.

C. Simple harmonic motion trajectory

The wheels in this section are considered to perform their rotation according to simple harmonic motion scenario. The two wheels are considered to undergo their motion in two opposite direction. The motion of the two wheels has the following characteristics: 0.1 frequency, 10 degree amplitude and 0 signal offset.

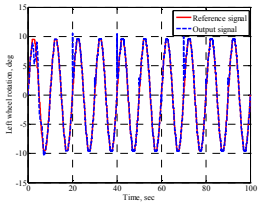

(a)

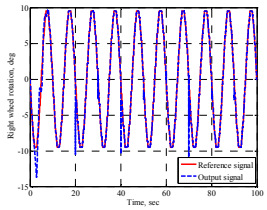

(b)

Fig. 25 Wheels angular motion versus reference trajectory

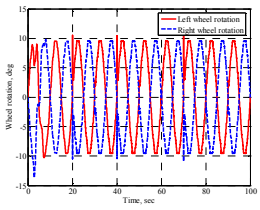

Fig. 26 Wheels angular motion

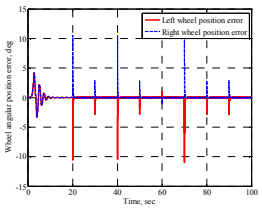

Fig. 27 Wheels position error

Both wheels are considered to undergo multiple cycles of continuous rotation, shown in Figures 25 (a) and 25(b), with a limit of 10 degrees in the form of a sine wave for the entire universe of discourse.

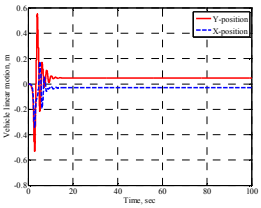

Fig. 28 Vehicle linear motion

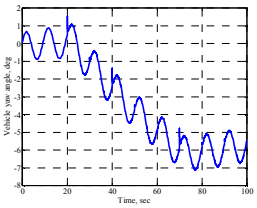

Fig. 29 Vehicle yaw angle

The developed control technique succeeded to track the assigned signal of wheels rotation as can be noticed In Figure 26 with the corresponding errors shown in Figure 27. As a result of the continuous motion of the two wheels in the previous manner, the vehicle undergoes a planar translational motion as shown in Figure 28 and a spinning motion about the vertical Z axis as shown in Figure 29. The vehicle will continue undergoing multiple periods of spinning as long as the two wheels are still rotating according to the mentioned scenario.

VII. CONCLUSIONS

The work presented a novel design of a two-wheeled vehicle with an extended rod. Adding a linear actuator to connect both parts of the IB gives the vehicle an additional degree of freedom. As for the mechanical design, investigations have been carried out for the vehicle in the static condition to help in adjusting the stand up angle and its related geometrical parameters. An investigation has been carried out on the steering behavior of the vehicle. The system model has been derived based on Lagrangian based dynamics. The dynamic equations have been described in terms of the partial angular movements of the vehicle wheels rather than the displacement of the centre of the vehicle. This has allowed designing a control strategy based on the actual measurements of the wheels rotations where two control signals are developed to activate, independently, each driving motor. In order to check the capability of the control strategies, the system has been tested utilizing three different motion scenarios of the wheels. The results have shown that the control technique used was able to achieve the target orientation of the whole system within less than 10 seconds while achieving the system balance in the upright position. The control strategy showed the capability to maneuver the vehicle using feedback of both the angular orientations of the left and right wheels. The developed control strategy was able to track, efficiently, the desired trajectories assigned to both wheels.

APPENDIX

$C_1 = M_l L_l^2 + M_a L_a^2$, $C_2 = L_l$, $C_3 = L_a = 2L_l$, $C_4 = 2L_l + L_u$,

$C_5 = 2L_l + 2L_u$, $C_6 = M_l L_l + M_a L_a$, $C = C_6 + M_u C_4 + MC_5$,

$C_7 = M_l / M_{eq}^2$, $C_8 = C_6 + M_u C_4 + MC_5 - M_{eq} L_l$, $C_9 = M_u + M$,

$C_{10} = M_a / M_{eq}^2$,

$C_{11} = C_6 + M_u C_4 + MC_5 - M_{eq} L_a$,

$C_{12} = M_u / M_{eq}^2$, $C_{13} = C_6 + M_u C_4 + MC_5 - M_{eq} C_4$, $C_{14} = M / M_{eq}^2$,

$C_{15} = -C_6 - M_u C_4 - MC_5 + M_{eq} C_5$,

$C_{16} = C_7 C_8^2 + C_{10} C_{11}^2 + C_{12} C_{13}^2 + C_{14} C_{15}^2$,

$C_{17} = 2C_7 C_8 C_9 + 2C_9 C_{10} C_{11} + 2C_{12} C_{13} \left(M_u + M - M_{eq}\right)$

$+ 2C_{14} C_{15} \left(M_{eq} - M_u - M\right)$

$C_{18} = C_7 C_9^2 + 2C_9^2 C_{10} + C_{12} \left(M_u + M - M_{eq}\right)^2 + C_{14} \left(M_{eq} - M_u - M\right)^2$

$C_{19} = C_{16} + M_u C_4^2 + MC_5^2$, $C_{20} = C_{17} + 2M_u C_4 + 2MC_5$

$C_{21} = C_{18} + C_9$, and $C_{22} = C_1 + C_{19}$.

REFERENCES

[1] ference on Robotics and Automation, Pasadena, CA, USA, May 19-23, 2008.

[2] Goher K M and Tokhi M.O., " Balance Control of a TWRM with a Dynamic Payload " The 11th International Conference on Climbing and Walking Robots and the support Technologies for Mobile Machines (CLAWAR 2008), The University of Coimbra, Coimbra, Portugal, September 8-10, 2008.

[3] Goher K M and Tokhi M.O., "A Two-Wheeled Vehicle with an Extended Rod, A Theoretical Approach", The 3rd International Conference on Modeling, Simulation and Applied Optimization (ICMSAO'09), American University of Sharjah, Sharjah, United Arab of Emirates, January 20-22, 2009.

[4] Goher K M and Tokhi M.O., A two-wheeled vehicle with an extended rod, mechanical design clues and dynamic modeling, in the Proceedings of the 8th IEEE International Conference on Cybernetic Intelligent Systems, Birmingham, UK, September 9-10., (2009).

[5] Goher K M and Tokhi M.O., "GA-Optimised Steering and Position Control a Two Wheeled Vehicle with an Extended Rod – A Simulation Study" The 12th International Conference on Climbing and Walking Robots and the support Technologies for Mobile Machines (CLAWAR 2009), Istanbul, Turkey, September 9-11, 2009.

[6] Goher K M and Tokhi M.O., "Genetic Algorithm based Modeling and Control of a Two Wheeled Vehicle with an Extended Rod, a Lagrangian based Dynamic Approach" The 8th IEEE International Conference on Cybernetic Intelligent Systems 2009, University of Birmingham, Birmingham, UK, September, 9-10, 2009.

[7] Goher K M and Tokhi M.O., A differentially steered two - wheeled vehicle with an extended rod: An investigation on the impact of wheels trajectory. in the Proceedings of the 13th International Conference on Climbing and Walking Robots and the Support Technologies for Mobile Machines (CLAWAR 2010), Nagoya, Japan, 31 August - 3 Sept 2010.

[8] Imamura R, Takei T, Yuta S, "Sensor Drift Compensation and Control of a Wheeled Inverted Pendulum Mobile Robot", 978-1-4244-1703-2/08/$25.00 ©2008 IEEE.

[9] Jeong S H and Takahashi T, "Wheeled Inverted Pendulum Type Assistant Robot: Inverted Mobile, Standing, and Sitting Motions" Proceedings of the 2007 IEEE/RSJ International Conference on Intelligent Robots and Systems, San Diego, CA, USA, Oct 29 - Nov 2, 2007.

[10] Jingtao Li et al, "Mechanical Design and Dynamic Modeling of a Two-Wheeled Inverted Pendulum Mobile Robot", Proceedings of the IEEE International Conference on Automation and Logistics, August 18 - 21, 2007, Jinan, China

[11] Nawawi S. W., Ahmad M. N. and Osman J. H. S., "Development of a Two-Wheeled Inverted Pendulum Mobile Robot", The 5th Student Conference on Research and Development -SCOReD 2007, 11-12 December 2007, Malaysia.

[12] Nawawi S.W, Ahmad M.N, Osman J.H.S, "Control of Two-wheels Inverted Pendulum Mobile Robot Using Full Order Sliding Mode Control", Proceedings of International Conference on Man-Machine Systems 2006, September 15-16 2006, Langkawi, Malaysia.

[13] Zheng C et al, "Mechanical Design and Control System of a Miniature Autonomous Surveillance Robot", Proceedings of the 2007 IEEE International Conference on Mechatronics and Automation,August5-8,2007,Harbin,China.

[14] Tsai C. C., Lin S.C. and Luo W.L. "Adaptive Steering of a Self-balancing Two-wheeled Transporter", Proceedings of 2006 CACS Automatic Control Conference, St. John's University,Tamsui, Taiwan, Nov. 10-11, 2006.

[15] Zhong W. and Helmut R¨ock H. "Energy and Passivity Based Control of the Double Inverted Pendulum on a Cart", Proceedings of the 2001 IEEE International Conference on Control Applications, Mexico city, Mexico, Sept. 5-7, 2001.